Biosensors and Bioelectronics 137 (2019) 96–109

Contents lists available at ScienceDirect

Biosensors and Bioelectronics

journal homepage: www.elsevier.com/locate/bios

Progress in biosensor based on DNA-templated copper nanoparticles

Zhihe Qing[a,*], Ailing Bai[a], Shuohui Xing[a], Zhen Zou[a,b], Xiaoxiao He[b], Kemin Wang[b], Ronghua Yang[a,b,**]

[a] Hunan Provincial Key Laboratory of Materials Protection for Electric Power and Transportation, Hunan Provincial Engineering Research Center for Food Processing of Aquatic Biotic Resources, School of Chemistry and Food Engineering, Changsha University of Science and Technology, Changsha, 410114, PR China
[b] State Key Laboratory of Chemo/Biosensing and Chemometrics, College of Chemistry and Chemical Engineering, College of Biology, Key Laboratory for Bio-Nanotechnology and Molecular Engineering of Hunan Province, Hunan University, Changsha, 410082, People's Republic of China

ARTICLE INFO

Keywords:
Biosensor
DNA
Template
Copper nanoparticles

ABSTRACT

During the last decades, by virtue of their unique physicochemical properties and potential application in microelectronics, biosensing and biomedicine, metal nanomaterials (MNs) have attracted great research interest and been highly developed. Deoxyribonucleic acid (DNA) is a particularly interesting ligand for templating bottom-up nanopreparation, by virtue of its excellent properties including nanosized geometry structure, programmable and artificial synthesis, DNA-metal ion interaction and powerful molecular recognition. DNA-templated copper nanoparticles (DNA-CuNPs) has been developed in recent years. Because of its advantages including simple and rapid preparation, high efficiency, MegaStokes shifting and low biological toxicity, DNA-CuNPs has been highly exploited for biochemical sensing from 2010, especially as a label-free detection manner, holding advantages in multiple analytical technologies including fluorescence, electrochemistry, surface plasmon resonance, inductively coupled plasma mass spectrometry and surface enhanced Raman spectroscopy. This review comprehensively tracks the preparation of DNA-CuNPs and its application in biosensing, and highlights the potential development and challenges regarding this field, aiming to promote the advance of this fertile research area.

1. Introduction

During the last decades, by virtue of their unique physicochemical properties and application potential in wide fields including microelectronics, biosensing and biomedicine, metal nanomaterials (MNs) have attracted great research interest and been highly developed (Zhang and Wang, 2014; Shang et al., 2011; Li et al., 2014; Tao et al., 2015; Jiang et al., 2018; Becerril and Woolley, 2009; Tanaka et al., 2011). Toward the synthesis of metal nanomaterials, bottom-up fabrications provide more flexible preparations in comparison to top-down approaches. Especially, as a precise manner to tune nanocrystal growth at atomic and molecular levels, biomolecules (e.g. DNA, protein, amino acid and sulfhydryl compound)-templated bottom-up nanopreparation has been developed and intensively studied (Xie et al., 2009; Wu et al., 2010; Retnakumari et al., 2010; Wang et al., 2013a; Jia et al., 2013, 2014; Ling et al., 2014; Goswami et al., 2011). Among many biomolecules available, deoxyribonucleic acid (DNA) is a particularly interesting ligand for template systems because of its excellent characteristics (Han and Wang, 2012; Liu, 2014; Kennedy et al., 2012; Chen et al., 2018a; Gwinn et al., 2008; Yang et al., 2016; Zhu et al., 2017), including (1) Nanosized structure. DNA is an easily available biopolymer composed of four deoxyribonucleotides (A, T, G, C) that are connected to one another through phosphodiester bond. Its physical size is at nanoscale dimension, as well known, the helix structure of double-stranded DNA (dsDNA) holds a ladder length of 0.34 nm per nucleotide and a width of 2 nm (Wing et al., 1980). Thus, one can see that the nanosized structure of DNA meet at the same dimension level of metal nanomaterials. (2) Programmable and artificial synthesis. To date, DNA with an arbitrary sequence or length can be artificially synthesized by an automatic synthesizer in high quality and large production, with a relatively low cost. External functional groups (fluorophore, quencher, thiol, alkyne, azide, etc.) can be grafted on nucleotides and integrated at will into DNA strands, providing additional properties that are significant for site-specific post

* Corresponding author.
** Corresponding author. Hunan Provincial Key Laboratory of Materials Protection for Electric Power and Transportation, Hunan Provincial Engineering Research Center for Food Processing of Aquatic Biotic Resources, School of Chemistry and Food Engineering, Changsha University of Science and Technology, Changsha, 410114, PR China.
E-mail addresses: qingzhihe@hnu.edu.cn (Z. Qing), Yangrh@pku.edu.cn (R. Yang).

https://doi.org/10.1016/j.bios.2019.05.014
Received 8 April 2019; Accepted 6 May 2019
Available online 07 May 2019
0956-5663/

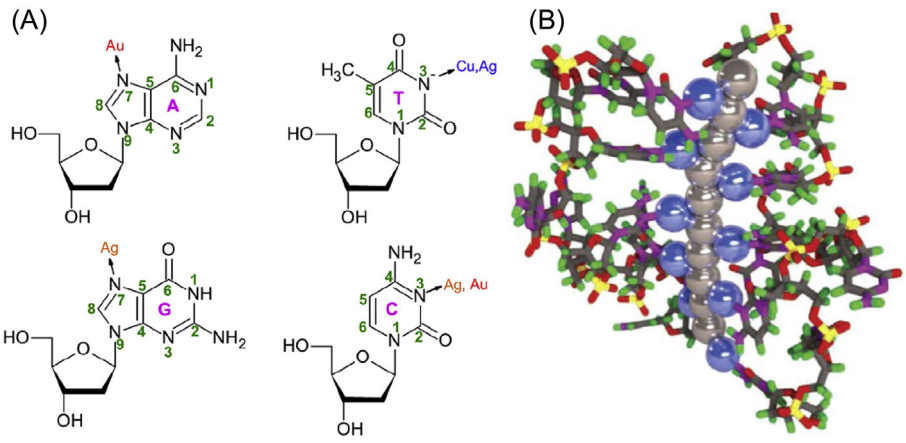

Fig. 1. (A) Chemical structures of DNA nucleosides and primary metal-coordination sites. (Reproduced with permission from Ref. (Liu, 2014). Copyright 2014, Elsevier B.V.). (B) The rod-like model of AgNCs with neutral Ag atoms (gray balls) and Ag^+ cations (blue balls) in poly-C DNA. (Reproduced with permission from Ref. (Schultz et al., 2013). Copyright 2013, Wiley-VCH). (For interpretation of the references to color in this figure legend, the reader is referred to the Web version of this article.)

Table 1
Physicochemical properties of different DNA-template MNs.

Type	Template	Synthesis time	Operating conditions	Stokes shift	Cost	Ref
Cu NMs	dsDNA	10 min	Room temperature	~260 nm	7 $·kg^{-1}(Cu)	Rotaru et al. (2010)
	Poly T	5 min	Room temperature	~275 nm	7 $·kg^{-1}(Cu)	Qing et al. (2013a)
Ag NMs	ssDNA	12 h	Cooling to 0 °C and vigorous shaking	~78 nm	600 $·kg^{-1}(Ag)	Petty et al. (2004)
	Poly C	12 h	Cooling to 0 °C and vigorous shaking	~50 nm	600 $·kg^{-1}(Ag)	Vosch et al. (2007)
	ssDNA	26 h	Shaking in dark	~60 nm	600 $·kg^{-1}(Ag)	Zhang et al. (2014)
Au NMs	ssDNA	46 h	Dark	~258 nm	43000 $·kg^{-1}(Au)	Liu et al. (2012a)
	Poly A	36 h	Dark	~185 nm	43000 $·kg^{-1}(Au)	Lin et al. (2015)
	Poly C/Poly A	24 h	Low pH, dark	~80 nm	43000 $·kg^{-1}(Au)	Kennedy et al. (2012)
PbS NMs	dsDNA	82 h	Shaking and heating	~89 nm	3.1 $·kg^{-1}(Pb)	Su and Gao (2013)
ZnS NMs	dsDNA	34 h	Shaking and heating	~128 nm	3.1 $·kg^{-1}(Zn)	Su et al. (2013)

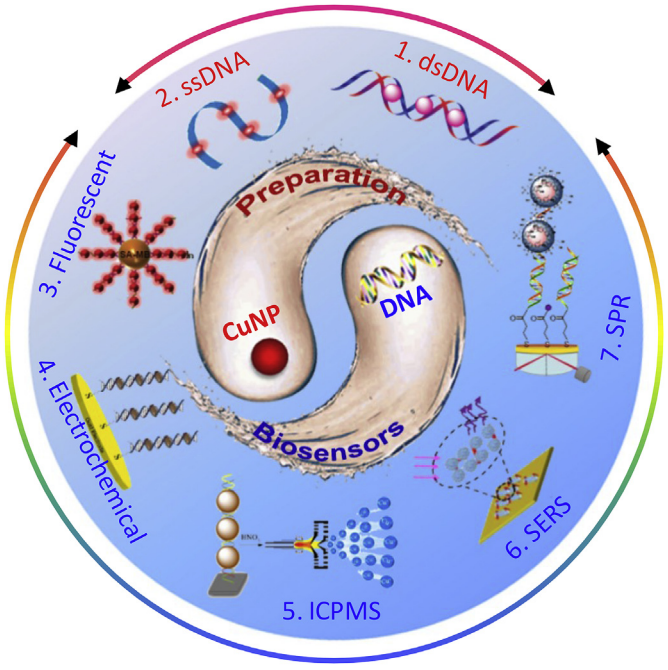

Scheme 1. Schematic illustration of preparation of DNA-CuNP and its application for biosensor development. Parts 3 reproduced with permission from Ref. (Hu et al., 2015). Copyright Royal Society of Chemistry. Parts 4 and 7 reproduced with permission from Ref. (Chen et al., 2018b) and Ref. (Yuan et al., 2017). Copyright Elsevier B.V. Part 5 and 6 reproduced with permission from Ref. (Liu et al., 2017) and (Zhou et al., 2016a). Copyright American Chemical Society.

functionalization and signal transduction. (3) DNA-metal ion interaction. From the chemical structure of DNA, it consists of negatively charged phosphate skeleton and nitrogenated nucleobases, conferring multiple binding sites for metal cations via electrostatic or coordination interactions (Fig. 1A) (Liu, 2014). DNA–metal ion interaction is the initial step of each DNA-templated heterogeneous nucleation process, metal nanomaterials can be formed on DNA scaffold (Fig. 1B) (Schultz et al., 2013), as a function of the addition of reducing agents (sodium borohydride, chalcogenide, sodium ascorbate and hydroxide, etc.), and different interactions between metal ions and DNA ligands can lead to the formation of diverse metal nanomaterials. (4) DNA plays an important role in molecular recognition (Wang et al., 2009; Zhu et al., 2013; Liu and Lu, 2007; Zheng et al., 2015a; Qing et al., 2017a, 2018). Routinely, it can used to construct probes for detection of nucleic acids based on complementary pairing of bases. DNA aptamer has been exploited as a kind of recognition unit, which is reasoningly called as chemical antibody (Ng et al., 2006). In principle, a corresponding aptamer can be selected toward any analyte by SELEX (systematic evolution of ligands by exponential enrichment) (Fang and Tan, 2009). Thus, taking advantage of the combination of molecular recognition and MNs-templating properties of DNA, a diverse range of biosensing modalities can be developed through skillfully designing DNA strands (Liu, 2014; Chen et al., 2018a). (5) Last but not least, DNA-templated MNs are relatively lower toxicity than conventional optical metal-containing nanomaterials (e.g. semiconductor quantum dots) (Plastino et al., 1999; Zhu et al., 2015a; Koval et al., 2006). And unlike organic fluorophores, *in situ* formed MNs do not require tediously covalent modifications on DNA, leading to lower cost in preparation.

Among DNA-templated MNs, copper nanoparticles (CuNPs) has been developed as a kind of relatively new alternative, double stranded DNA-templated CuNPs (dsDNA-CuNPs) was first reported by Mokhir et al., in 2010 (Rotaru et al., 2010), and single stranded poly(thymine)-templated CuNPs (poly T-CuNPs) was pioneered by us in 2013 (Qing et al., 2013a). Interestingly, DNA-CuNPs display distinctive advantages

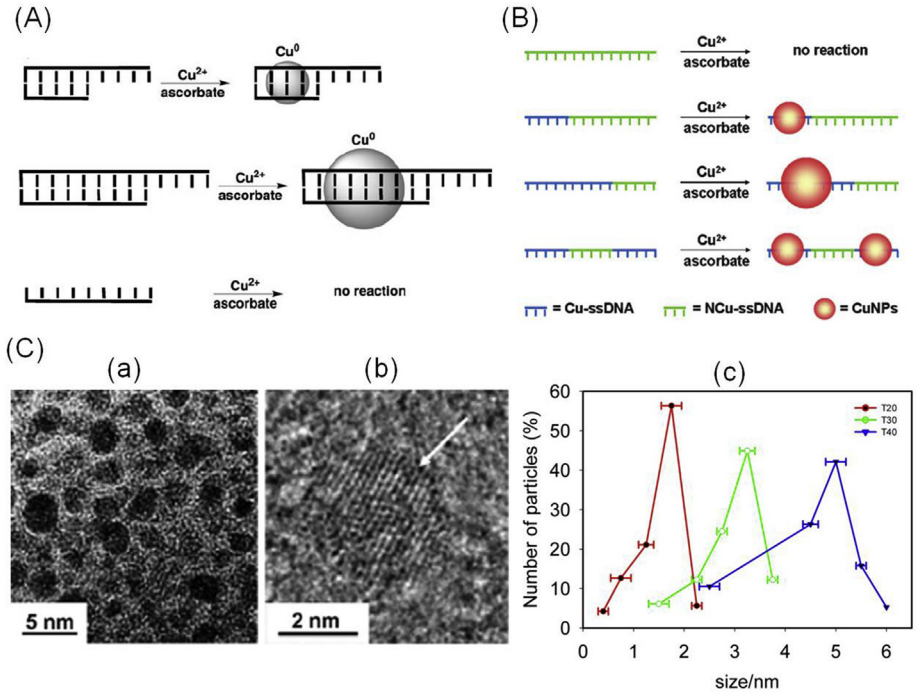

Fig. 2. DNA sequence-dependent formation of CuNPs. (A) The formation of fluorescent CuNPs templated by dsDNA. (Reproduced with permission from Ref. (Rotaru et al., 2010). Copyright 2010, Wiley-VCH). (B) The formation of fluorescent CuNPs templated by ssDNA. Poly(thymine) (Poly T) was screened as a single-stranded template for the formation of fluorescent CuNPs. (Reproduced with permission from Ref. (Qing et al., 2013a). Copyright 2010, Wiley-VCH). (C) Shape and size characterizations of Poly T-templated CuNPs: TEM image of CuNPs (a), high-resolution image of the crystal lattice (b), and the relationship between size distribution and the length of poly-T.

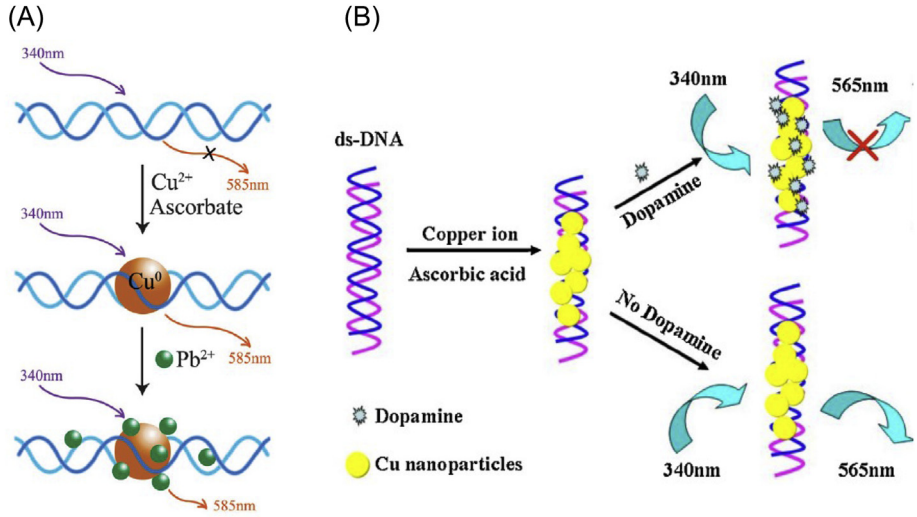

Fig. 3. DNA-CuNPs-biosensors for detecting reactive quenchers. (A) Pb^{2+} detection. (Reproduced with permission from Ref. (Chen et al., 2012). Copyright 2012, Royal Society of Chemistry). (B) Dopamina detection based on their direct quenching effects on dsDNA-CuNPs. (Reproduced with permission from Ref. (Wang et al., 2015a). Copyright 2015, Elsevier B.V.).

in preparation and application, some physicochemical parameters of DNA-CuNPs are summarized in Table 1. The synthesis of DNA-CuNPs is very simple, efficient and rapid under mild conditions, with low-cost and without any complicated manipulation. There is a MegaStokes shifting (~270 nm) in its fluorescence emission whose intensity is proportional to the length of DNA templates. In addition, due to copper's role as micronutrient for living systems, copper nanomaterials are more biocompatible and environmentally friendly than other heavy-metal nanomaterials. Therefore, DNA-CuNPs as an *in situ* synthetic nanoprobe holds great potential for wide applications in developing biosensors.

In the past few years, the research on DNA-CuNPs and its applications in biosensor development is a rapidly growing field, there are more and more reports on this topic. In the hand of the detected targets, they include ions detection, small biomolecules detection, biomacromolecules detection, cell analysis and logic circuit construction; In the hand of the used analytical technologies, they include fluorescence, electrochemistry, surface plasmon resonance (SPR), surface enhanced Raman spectroscopy (SERS), and inductively coupled plasma mass spectrometry (ICPMS) assay. Here, based on our previous studies on optical inorganic metal nanoparticles, especially DNA-template MNs, we here review recent progress in development of DNA-CuNPs and its application for biosensing (Scheme 1), we also discuss the mechanistic understanding, the advantages and limitations in different aspects, which may facilitate the trend in future research and application of this new optical materials.

2. Preparation of DNA-templated CuNPs

Because of their small diameter and high surface energy, MNs tend to be physically agglomerated, thus, a ligand or a matrix is needed for stabilizing fluorescent MNs in aqueous solution. In 2004, as the initial discovery of connection between fluorescent MNs and DNA, Dickson group found that single-stranded cytosine (C)-rich DNA can template silver nanoclusters (AgNCs), by virtue of a specific and strong coordination between Ag^{+} the N3 of cytosine (Petty et al., 2004).

Table 2
Biosensors based on reactive quenchers on DNA-CuNPs.

Target	Template type	Template length/bp	Read out	λem/nm (λex)/nm	Detection time/min	Detection limit	Linear range	Real sample	Ref
S2-	dsDNA	–	Turn-off	585 (340)	5	80 nM	2–20 μM	River water	Liu et al. (2012b)
Pb2+	dsDNA	35	Turn-off	585 (340)	5	5 nM	5–100 nM	Human urine and river water	Chen et al. (2012)
Pb2+	Poly T	30	Turn-off	615 (340)	10	0.4 nM	1–500 nM	Tap water	Ou et al. (2014)
Biothiols	dsDNA	32	Turn-off	580 (340)	3	2 μM (Cys)	2.0×10^{-6}–1.0×10^{-4} M	Human plasma	Hu et al. (2013a)
						2 μM (GSH)	2.0×10^{-6}–8.0×10^{-5} M		
						5 μM (Hcy)	5.0×10^{-6}–2.0×10^{-4} M		
Cysteine	Poly T	30	Turn-off	610 (340)	10	7.3 μM	12.5–100 μM	Medicine	Peng et al. (2017)
Dopamine	dsDNA	25	Turn-off	565 (340)	5	20 pM	0.1–10000 nM	Dopamine hydrochloride injection	Wang et al. (2015a)
I-	Poly T	–	Turn-off	637 (345)	–	15 nM	0.05–80 μM	Kunming mice extract fluid	Chen et al. (2017)
Trypsin	Poly T	30	Turn-off	615 (340)	30	42 ng mL^{-1}	0.25–1000 ng mL^{-1}	–	Ou et al. (2015)
Glucose	dsDNA	25	Turn-off	565 (340)	30	12 nM	0.05–100 μM	Serum	Wang et al. (2015b)
TNP	Poly T	50	Turn-off	627 (340)	30	0.03 μM	0.1–100 μM	Natural water	Li et al. (2016)

Subsequent studies demonstrated that four nucleotides (A, T, G and C) play a part in the formation of MNs, there is at least one metal-binding site on each base (Liu, 2014). The connection between fluorescent CuNPs and short DNA was first been reported by Mokhir group in 2010 (Fig. 2A) (Rotaru et al., 2010). dsDNA can template the formation of fluorescent CuNPs, through initial reduction of Cu^{2+} and then binding to the hard Lewis bases (oxygen atoms) or intermediate Lewis bases (nitrogen atoms); the major groove of the dsDNA plays an important role in the formation of fluorescent CuNPs, which is blocked in the triplex and which is absent in the ssDNA, the size of the nanoparticles formed is proportional to the number of base pairs in the dsDNA template; in addition, the charge of the dsDNA also seems to be very important, as less-charged peptide nucleic acid (PNA)/DNA duplexes are inoperative at all (Rotaru et al., 2010). Subsequently, we and Ouyang group systematically investigated the sequence-dependence of dsDNA-templated fluorescent CuNPs. Poly(AT-TA) is found as the specific sequence composition which contributes to this formation, and the formation efficiency is highly dependent on the length and polymerization degree of poly(AT-TA) dsDNA (Qing et al., 2014a; Song et al., 2015).

As a contribution to the development of DNA-templated fluorescent CuNPs, we firstly discovered the relationship between ssDNA and the formation of fluorescent CuNPs in 2013 (Fig. 2B) (Qing et al., 2013a). Poly(thymine) (Poly T) was screened as a single-stranded template for the formation of fluorescent CuNPs, due to that there are binding interactions between thymine and Cu^{2+} ions and the thymine-complexed Cu^{2+} are reduced to Cu^0 by reducing agents along the contour of the poly T template. The formation of poly T-templated CuNPs can be carried out in different buffers including MOPS, PBS and HEPES, except for Tris buffer; Contrary to sodium borohydride and sodium citrate which are frequently used in synthesis of MNs, sodium ascorbate displays high effeciency to catalyze this conversion reaction from Cu^{2+} to fluorescent poly T-templated CuNPs (Qing et al., 2016a). Acidic condition is disadvantageous for the formation of fluorescent CuNPs, while weak alkali from pH 7.0 to 9.8 is advantageous; A moderate ion strength (e.g. 150 mM NaCl) is favorable for this formation; Lower temperature results in higher fluorescence and the reaction for signal formation is fast, completing with several minutes (Qing et al., 2014b). The shape of Poly T-templated CuNPs is similar to bead, the size of Poly T-templated CuNPs can be simply regulated by altering the length of the poly T (Fig. 2C). In addition, other ssDNAs, such as random ssDNA, poly (adenine) (poly A), poly(cytosine) (poly C), and poly(guanine) (poly G) failed to serve as templates for fluorescent CuNPs under the same conditions, selective metallization of ssDNA gave nanostructures with alternating metallized and non-metallized parts using poly T as a template for CuNPs formation and other ssDNAs as linkers. Because the non-metallized segments can be pre-designed, they can be conveniently connected with other objects or immobilized on surfaces, which is also important for the construction of biosensors, especially electrochemical assays.

Thus, these unique physicochemical properties and excellences in preparation make DNA-templated CuNPs as an excellent alternative to traditional signal reporters. Besides the extraordinary application in fluorescent sensor development, it also holds good potential for exploiting other sensors of various analytical technologies including electrochemistry, SPR, SERS and ICPMS.

3. Biosensors facilitated by DNA-CuNPs

3.1. Fluorescent biosensors

DNA-CuNPs has obvious advantages in preparation including simplicity, rapidity and efficiency, and good fluorescence properties including MegaStokes shifting, sequence-dependence and length-dependence. Thus, since the first report of DNA-CuNPs by Mokhir et al., fluorescence property of this emerging nanomaterials has been intently used to construct biosensors. Many fluorescent strategies and methods

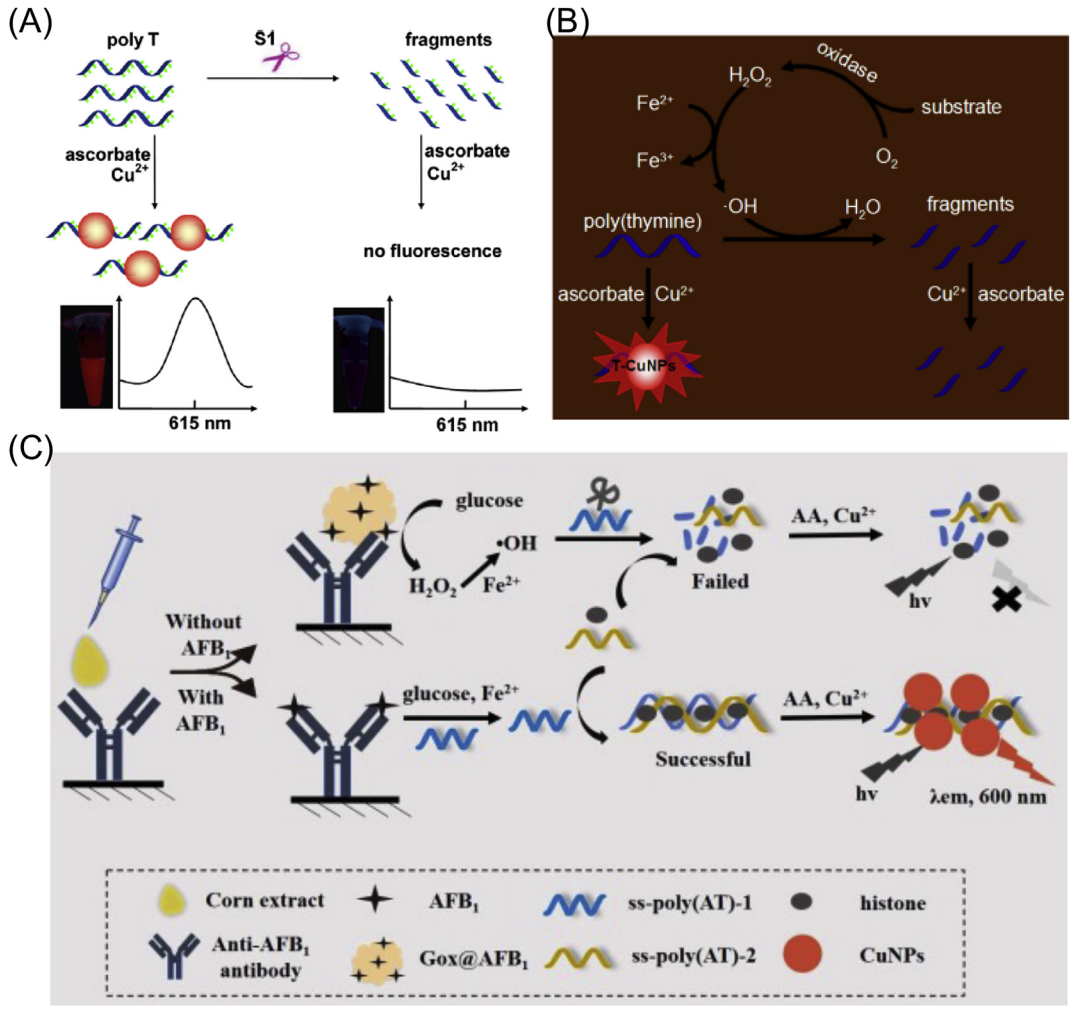

Fig. 4. DNA-CuNPs-biosensors based on length modulation of templates. (A) nuclease assay based on target-triggered degradation of poly T. (Reproduced with permission from Ref. (Qing et al., 2013b). Copyright 2013, American Chemical Society). (B) biosensor for hydrogen peroxide (H_2O_2) and substrates of oxidases based on hydroxyl radical (·OH)-mediated oxidative cleavage of poly T. (Reproduced with permission from Ref. (Mao et al., 2015). Copyright 2015, American Chemical Society). (C) immunoassay based on the enzyme cleaving ss-DNA to regulate the synthesis of dsDNA-CuNPs. (Reproduced with permission from Ref. (Xiong et al., 2018). Copyright 2018, Royal Society of Chemistry).

have been developed for detection of wide range targets, including ions, small biological molecules and biomacromolecules. Here, we review the progress in this respect by dividing it into four categories, according to different signaling mechanisms.

3.1.1. Signaling based on reactive quenchers

Because of high specific area of MNs, most metal atoms in an MN are exposed to an external environment, where other chemicals can facilely interact with the surface of MNs. The interface chemical reactions can result in changes in fluorescence emission, providing detectable signal for constructing fluorescent biosensors. Early works on this were reported by Zeng and co-workers, direct quenching effects on dsDNA-CuNPs were found from S^{2-} anions and Pb^{2+} cation (Fig. 3A), and simple methods were developed for the detection of these two ions in aqueous solution by using dsDNA-CuNPs as novel fluorescence probes, with high selectivity and sensitivity (Liu et al., 2012b; Chen et al., 2012). Later, Chu group developed an ultrasensitive and label-free strategy for Pb^{2+} detection based on its quenching effect on poly T-CuNPs, a high sensitivity (LOD 0.4 nM) was achieved (Ou et al., 2014). This signaling mechanism was also exploited to detect biological molecules. Hu et al. reported a simple and sensitive method for the detection of biothiols including glutathione (GSH), cysteine (Cys) and homocysteine (Hcy), based on the formation of nonfluorescent coordination complexes between the dsDNA-CuNPs and biothiols (Hu et al., 2013a). Peng et al. also proposed a highly selective and rapid analytical method to detect cysteine in aqueous solution, by using poly T-CuNPs (Peng et al., 2017). Wang and co-workers developed a label-free and ultrasensitive fluorescent sensor for dopamine detection based on the direct quenching effect resulting from the formation of photo-induced electron transfer process between dopamine and CuNPs (Fig. 3B) (Wang et al., 2015a). Tang group reported a fast, highly sensitive and selective assay of iodide ions with poly T-CuNPs as a fluorescent probe, due to the instant quenching of the fluorescence of poly T-CuNPs by iodide ion (Chen et al., 2017). Besides direct quenching-mediated detection, some biosensor were also developed based on indirect quenching, in which a target induced the production of a intermediate molecule that can quench the fluorescence of DNA-CuNPs, realizing indirect detection of the target. Ou et al. developed a simple and sensitive fluorescent assay for trypsin based on poly T-CuNPs and its response to trypsin-catalyzed hydrolysis of cytochrome C, in which free cysteine residues are released and quench the fluorescence of poly T-CuNPs (Ou et al., 2015). H_2O_2-mediated fluorescence quenching of dsDNA-CuNPs for label-free and sensitive detection of glucose was proposed by Wang et al. (2015b). This category is simple in operation and cost-effective, generally with good detection performance. Biosensors based on reactive quenchers on DNA-CuNPs are

Table 3
Biosensors based on length modulation of templates.

Target	Template type	Modulation mechanization	Read out	λem/nm (λex)/nm	Detection time (min)	Detection limit	Linear range	Real sample	Ref
Nuclease	Poly T	Enzymatic cleavage	Turn-off	615 (340)	5	5×10^{-7} U·μL^{-1}	5×10^{-6}–2×10^{-3} U·μL^{-1}	Cell medium	Qing et al. (2013b)
H_2O_2	Poly T	Oxidase-catalyzed oxidation reaction	Turn-off	615 (340)	10	0.05 nM	0.05–1.6 nM	Serum	Mao et al. (2015)
Enzymes	Dumbbell DNA	Enzymatic cleavage	Turn-on	600 (340)	50	1 U·mL^{-1} (T4 ligase) 0.05 U·mL^{-1} (T4 PNK)	1–50 U·mL^{-1} (T4 ligase) 0.05–5 U·mL^{-1} (T4 PNK)	Cell extract	Qing et al. (2017b)
DNase I	Poly T	Enzymatic polymerization	Turn-on	615 (340)	5	0.02 U·mL^{-1}	0.02–2 U·mL^{-1}	Cell medium	Luo et al. (2017)
PNK	dsDNA	Enzymatic cleavage	Turn-off	565 (340)	3	0.49 U·mL^{-1}	0–3 U·mL^{-1}	Cell extract	Zhang et al. (2013a)
Nuclease	dsDNA	Enzymatic cleavage	Turn-off	580(340)	10	0.3 U·mL^{-1}	1–50 U·mL^{-1}	–	Hu et al. (2013b)
SA	Poly T	Enzymatic cleavage	Turn-on	615 (340)	5	0.1 nM	0.5–1000 nM	Serum	Wang et al. (2015c)
ATP	Dumbbell DNA	Enzymatic cleavage	Turn-on	575 (343)	50	81 pM	0.1–125 nM	Serum	Chen et al. (2016)
ATP	Poly T	Enzymatic cleavage	Turn-on	615 (340)	10	93 nM	0.2–50 μM	Cell medium	Song et al. (2017a)
Actin	dsDNA	Enzymatic cleavage	Turn-on	585(340)	30	0.12 μg mL^{-1}	0–12 μg mL^{-1}	Cell medium	Song et al. (2017b)
AFB1	Poly AT	Oxidase-catalyzed oxidation reaction	Turn-on	600 (340)	80	0.15 pg mL^{-1}	0.46–400 pg mL^{-1}	Corn	Xiong et al. (2018)
Hg^{2+}	Poly T	Enzymatic cleavage	Turn-on	650 (340)	–	16 pM	50 pM–500 μM	Lake water	Li et al. (2018a)
Exo III	dsDNA	Enzymatic cleavage	Turn-off	575 (340)	10	0.02 U·mL^{-1}	0.05–2 U·mL^{-1}	Serum	Zhang et al. (2015a)
NAD^+	dsDNA	Enzymatic reaction	Turn-off	600 (340)	30	0.2 nM	0.2–20 nM	Cell extract	Ge et al. (2016a)
Dam MTase	dsDNA	Enzymatic cleavage	Turn-off	570 (340)	30	0.01 U·mL^{-1}	0.01–5 U·mL^{-1}	Serum	Lai et al. (2016)
ATP	Poly T	Enzymatic cleavage	Turn-on	615 (350)	20	500 nM	1–80 μM	Cell extract	Cai et al. (2017)
Protein	Poly T	Enzymatic reaction	Turn-off	617 (349)	120	2.4 nM (Thrombin) 1.3 nM (VEGF165)	10–400 nM (Thrombin) 10–80 nM (VEGF165)	–	Cao et al. (2017a)
Exo III	Poly T	Enzymatic cleavage	Turn-off	600 (340)	15	0.02 U·mL^{-1}	0.02–10 U·mL^{-1}	Cell extract	Ge et al. (2017)
MTase	Dumbbell DNA	Enzymatic cleavage	Turn-on	620 (350)	60	1.6968×10^{-4} U·μL^{-1}	0.1–0.2 U·μL^{-1}	Serum	Yin et al. (2018)
*Eco*RI	dsDNA	Enzymatic cleavage	Turn-off	575 (340)	100	0.00087 U·μL^{-1}	0.002–0.1 U·μL^{-1}	–	Zhao et al. (2017)
T4 PNK	Poly T	Enzymatic polymerization	Turn-on	600 (365)	–	0.01 U·mL^{-1}	0.012–0.175 U·mL^{-1}	–	He et al. (2015)
OTA	dsDNA	Enzymatic cleavage	Turn-off	570 (340)	90	5 ng mL^{-1}	0–0.1 μg mL^{-1}	Corn	Song et al. (2018a)

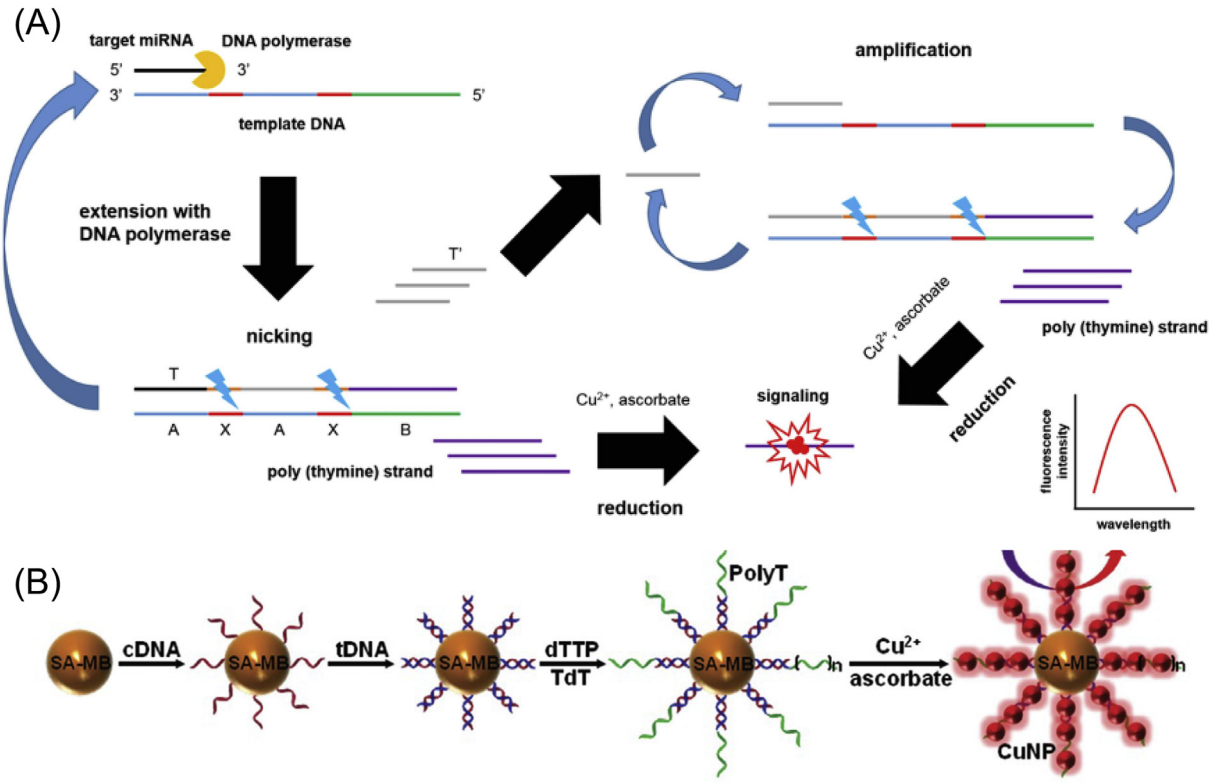

Fig. 5. DNA-CuNPs-biosensors based on quantity modulation of templates. (A) DNA detection through surface-initiated enzymatic generation of poly T. (Reproduced with permission from Ref. (Wang et al., 2017a). Copyright 2016, IOP Publishing Ltd). (B) microRNA detection via target-assisted isothermal exponential amplification generation of poly T. (Reproduced with permission from Ref. (Hu et al., 2015). Copyright 2015, Royal Society of Chemistry).

summarized in Table 2.

3.1.2. Signaling based on length modulation of templates

The formation of fluorescent DNA-CuNPs is highly DNA length-dependent, thus their fluorescence emission signal is proportional to the length of DNA templates, providing a useful signaling strategy for developing biosensors. We first exploited this strategy for biosensing in 2013 (Qing et al., 2013b), a label-free fluorescent method was developed for nuclease assay based on target-triggered degradation of poly T (Fig. 4A). the signal reporter of poly T of 30 mer (T30) kept the original long state in the absence of nuclease, which could effectively template the formation of fluorescent CuNPs. In the presence of nuclease, poly T was digested to mono- or oligonucleotide fragments with decrease of fluorescence. It was ultrasensitive for model nuclease S1 with a detectable minimum concentration of 5×10^{-7} units μL^{-1}. Soon afterwards, we proposed a fluorescent biosensor for hydrogen peroxide (H_2O_2) and substrates of oxidases based on hydroxyl radical (·OH)-mediated oxidative cleavage of poly T (Fig. 4B) (Mao et al., 2015). In the absence of H_2O_2, poly T could effectively template the formation of CuNPs with high fluorescence signal intensity, whereas decreased signal was detected when in the presence of H_2O_2, because Fenton reaction can convert H_2O_2 into ·OH that can destroy poly T. When a biological substrate is detected, H_2O_2 can be generated in oxidation process catalyzed by its oxidase, then lead to degradation of poly T and decrease of fluorescence signal. Further, for detection of ligase and polynucleotide kinase, a nano-fluorescent probe was also developed by us, when in the absence of both targets or presence of either target, the dumbbell DNA template would be digested by exonuclease, no fluorescence could be detected; while in the presence of both enzymes, dumbbell DNA could be locked and resist the cleavage of exonuclease, templating CuNPs with high fluorescence signal intensity (Qing et al., 2017b). We also developed a method for deoxyribonuclease (DNase) assay by terminal deoxynucleotidyl transferase (TDT)-catalyzed extending generation of poly T. when in the absence of the target, 3′-phosphorylated DNA primers could not be extended by TDT, when with the addition of DNase I, the primer could be cleavaged to generate 3′-hydroxylated fragments, which could further be extended by TDT in dTTP pool into superlong poly T ssDNA for CuNPs formation, with high fluorescence signal (Luo et al., 2017).

In addition, many biosensors based on this strategy was constructed by other groups. For example, Yu group developed methods for nuclease enzyme and polynucleotide kinase detection based on target-triggered length modulation of dsDNA templates (Zhang et al., 2013a; Hu et al., 2013b). Wang et al. developed a fluorescent platform for detection of ligand-protein interactions based on poly T-templated CuNPs and terminal protection of small molecule-linked DNA (Wang et al., 2015c). Sensitive detection of adenosine triphosphate (ATP) was achieved by Chen et al., based on multifunctional dumbbell-shaped DNA-templated formation of fluorescent CuNPs and target-induced protection of dumbbell DNA from enzymatic degradation (Chen et al., 2016). In Ouyang group, nuclease-assisted fluorometric assays for ATP and actin detection were developed based on length modulation of templates and *in situ* formation of fluorescent CuNPs (Song et al., 2017a, 2017b). Xiong et al. reported a fluorescence immunoassay platform based on the enzyme cleaving ssDNA to regulate the synthesis of dsDNA-templated CuNPs (Fig. 4C) (Xiong et al., 2018). Dai group achieved a high signal-to-noise ratio biosensor for toxic mercury ions (Hg^{2+}), based on fluorescence regulation of CuNPs via DNA template manipulation (Li et al., 2018a). Biosensors based on length modulation of templates are summarized in Table 3.

3.1.3. Signaling based on quantity modulation of templates

As demonstrated in previous works, the formation of CuNPs is highly influenced by the quantity of DNA templates, the fluorescence signal can be tuned through quantity modulation of templates. Based on this strategy, we exploited dsDNA-templated CuNPs as a “green” nano-

Table 4
Biosensors based on quantity modulation of templates.

Target	Template type	Modulation mechanization	Read out	λem/nm (λex)/nm	Detection time/min	Detection limit	Linear range	Real sample	Ref
KF/DNA	dsDNA	Enzymatic polymerization	Turn-on	570 (340)	–	1×10^{-5} U·μL^{-1} (KF) 0.13 aM (DNA)	1×10^{-5}–4×10^{-4} U·μL^{-1} (KF) 1 aM–10 pM (DNA)	–	Qing et al. (2014c)
MicroRNA	dsDNA	TEAR	Turn-on	608 (340)	–	1 pM	1 pM–10 nM	–	Wang et al. (2013b)
MicroRNA	Poly T	EPEPT	Turn-on	600 (340)	180	100 fM	1 pM–1 nM	Cell lysate	Chi et al. (2017)
MicroRNA	Poly T	TAIEA	Turn-on	600 (340)	60	0.27 fM	70 fM–700 nM	Cell lysate	Park et al. (2016)
ATP	dsDNA	TCSDA	Turn-on	598 (340)	5	5 pM	0.01–100 nM	–	Wang et al. (2017a)
Biotin-SA	Poly T	RCA	Turn-on	625 (340)	5	0.02 nM	0.0692–17.3 nM	Serum	He and Jiao (2018)
DNA	Poly T	Enzymatic polymerization	Turn-on	670 (340)	–	98.2 pM	0.1–10 nM	–	Hu et al. (2015)
ALP/*Bam*HI	Poly T	Enzymatic polymerization	Turn-on	625 (350)	–	0.052×10^{-3} U·mL^{-1}(ALP) 0.005 U·mL^{-1} (*Bam*HI)	0.052×10^{-3}–0.1 U·mL^{-1} (ALP) 0.05–20 U·mL^{-1} (*Bam*HI)	–	Peng et al. (2015)
T4 PNKP	Poly T	RCA	Turn-on	625 (340)	50	0.02 U·mL^{-1}	0.02–20 U·mL^{-1}	Cell extract	Ge et al. (2016b)
SA/Biotin	Poly T	Enzymatic polymerization	Turn-on	617 (349)	10	0.47 nM (SA) 3.1 nM (Biotin)	1–200 nM (SA) 10–2000 nM (Biotin)	Serum	Cao et al. (2017b)
TdT	Poly AT	Enzymatic polymerization	Turn-on	570 (340)	–	60 mU·L^{-1}	0.7–14 U·L^{-1}	Cell extract	Zhou et al. (2017)
MicroRNA	Poly T	Double amplification	Turn-on	625 (350)	120	20 pM	20–1000 pM	–	Xu et al. (2018)
DNA	Poly T	Cation-exchange reaction	Turn-on	625 (340)	90	6×10^{-12}M	1×10^{-11}–1×10^{-6}M	Serum	Song et al. (2018b)
DNA	Poly T	RCA	Turn-on	650 (340)	30	7.79 aM	10 aM–1 μM	Serum	Park et al. (2018)
PDGF-BB	dsDNA	Enzymatic polymerization	Turn-on	575 (340)	30	4 nM·L^{-1}	0–50 nM·L^{-1}	–	Yang et al. (2014)
MicroRNA	dsDNA	RCR	Turn-on	570 (340)	10	10 pM	10–400 pM	–	Xu et al. (2014)

dye for polymerization-mediated biosensors, because a great deal of dsDNA templates would be generated after polymerization reactions (e.g. polymerase chain reaction, PCR), good feasibility and universality were verified (Qing et al., 2014c). In addition, biosensors based on this signaling model were also constructed by other groups. For example, Wang et al. developed a simple and label-free strategy for microRNA (miRNAs) detection by using dsDNA-CuNPs as fluorescent signal reporters (Wang et al., 2013b). A relatively long DNA was designed to hybrize with the miRNA target, and could be amplified by isothermal enzymatic reaction, in which polymerases and nicking enzymes were used as mechanical activators, good sensitivity and specificity were achieved. For simple, rapid and sensitive detection of RNA, Qiu group reported another method in which short target miRNAs could be efficiently converted into long poly T sequences that can template the *in situ* formation of fluorescent CuNPs as signal reporter for detecting the target (Chi et al., 2017). Park et al. also deviaed a rapid and ultrasensitive method for miRNAs sensing (Fig. 5A) (Park et al., 2016), by taking advantage of target-triggered isothermal enzymatic exponential amplification and poly T-CuNPs as fluorescent signal indicators. High sensitivity and great potential towards real clinical applications were demonstrated. Else, Jiang group developed a aptamer-based fluorometric strategy biosensing, by combining target-cycling strand displacement amplification and synthesis of *in situ* formation of fluorescent dsDNA-CuNPs. ATP as a model target was detected, via target-induced structure switching design, this sensing scheme is applicable to many other targets for which suitable aptamers are obtained (Wang et al., 2017a). He and Jiao recently developed a highly sensitive and label-free fluorescent method for the detection of small molecule-protein interactions based on exonuclease III (Exo III)-aided DNA recycling amplification and poly T-CuNPs. Biotinylated dsDNA served as the trigger, a hairpin DNA which contained thymine-rich sequence and the trigger DNA recognition domain was designed as the signal reporter. With the small molecule-protein interaction and the assistance of Exo III digestion, the trigger strand could be used circularly to convert hairpin DNAs into poly T sequences that can template the formation of fluorescent CuNPs, good detection performance was demonstrated (He and Jiao, 2018). A DNA sensing strategy was also developed through surface-initiated enzymatic polymerization and poly T-CuNPs (Fig. 5B) (Hu et al., 2015). Biosensors based on quantity modulation of templates are summarized in Table 4.

3.1.4. Signaling based on microenvironment modulation

As found in investigation, photophysical properties of DNA-CuNPs are impressible to its microenvironment including the level of copper ion (Cu^{2+}), the concentration of mediators, the distance between DNA-CuNPs, and base difference, opening up a new path for construction of biosensors. Directly, based on the high-dependence of the level of Cu^{2+}, *in situ* formation of poly T-CuNPs was applied to developing simple and even portable method for Cu^{2+} detection by us (Fig. 6A) (Qing et al., 2014b). As shown in Figure, a striplike poly T-caged and microwell-printed hydrogel was designed to detect Cu^{2+}, uniform wells of microliter volume (microwells) were printed on the hydrogel's surface for sample-injection. When the injected sample was stained by Cu^{2+}, fluorescent CuNPs would be *in situ* templated by poly T in the hydrogel. With ultraviolet (UV) irradiation, the red fluorescence of CuNPs could be observed by naked-eye and recorded by a common camera without complicated instruments. This strategy integrated sample-injection, reaction and indication with fast signal response, providing an add-and-read manner for viaual and portable detection of Cu^{2+}. As well as a strip-like strategy, it has great potential and significance for popular monitoring of Cu^{2+} polution, especially in remote regions (Qing et al., 2014b; Li et al., 2019). Wang group found that fluorescence emission of DNA-CuNPs is highly sensitive to base type which is located in the major groove of dsDNA, then a powerful strategy for fluorescent identification of single nucleotide polymorphisms was developed (Fig. 6B) (Jia et al., 2012). In addition, Zhou et al. found that when the distance

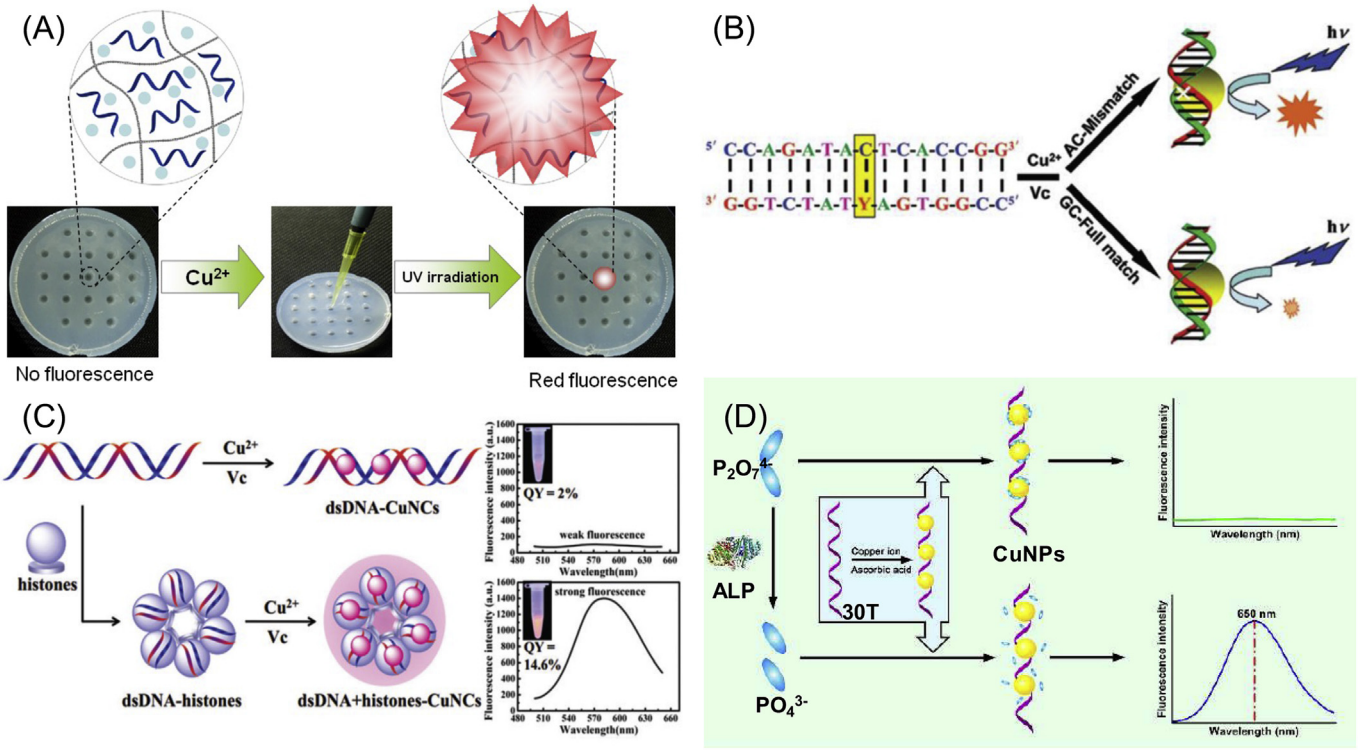

Fig. 6. DNA-CuNPs-biosensors based on microenvironment modulation. (A) Cu^{2+} detection based on a striplike poly T-caged and microwell-printed hydrogel (Reproduced with permission from Ref. (Qing et al., 2014b). Copyright 2014, American Chemical Society). (B) Fluorescent Identification of Single Nucleotide Polymorphisms based on dsDNA-CuNPs' different sensitivity to different base type located in the major groove (Reproduced with permission from Ref. (Jia et al., 2012). Copyright 2012, American Chemical Society). (C) Histone detection based on the fact that The histone–DNA interaction can greatly improve the fluorescence intensity of DNA-CuNPs (Reproduced with permission from Ref. (Lian et al., 2017). Copyright 2017, Royal Society of Chemistry). (D) ALP biosensor based on poly (30T)-templated CuNPs and an enzyme-triggered reaction (Reproduced with permission from Ref. (Li et al., 2017). Copyright 2017, American Chemical Society).

between different poly T-CuNPs was brought closely, their fluorescence could significantly enhanced, consequently, facile and label-free sensors for detecting biomarkers were constructed based on this phenomenon (Fig. 6C) (Zhou et al., 2016b) (Lian et al., 2017). Dai group recently used pyrophosphate ion (PPi) as a mediator to regulate the fluorescence of poly T-CuNPs, and enzymatic reaction to regulate the concentration of PPi, then a biosensor for alkaline phosphatase (ALP) was successfully developed, with a wide linear range, a low detection limit and a good potential for practical applications (Fig. 6D) (Li et al., 2017). Biosensors based on microenvironment modulation are summarized in Table 5.

3.1.5. Signaling based on quenching property of DNA-CuNPs

Besides its excellent fluorescence emission property, DNA-CuNPs' quenching effect on other fluorophores was first investigated by us in 2016 (Fig. 7) (Qing et al., 2016b). As found, DNA-CuNPs could quench the nucleic acid intercalating dye (a carbazole derivative, ethyl-4-[3,6-bis(1-methyl-4-vinylpyridium iodine)-9H-carbazol-9-yl] butanoate, EBMVC-B), and was exploited as an ideal fluorescence quencher in constructing a sensor for cyanide ion (CN^-). By virtue of CuNPs' small size and its high chemical reactivity with cyanide, CuNPs could be rapidly etched by CN^- via an Elsner-like reaction (Liu et al., 2010), with a significant decline in fluorescence intensity. A high selectivity was achieved for CN^- detection by the strategy, practical applications for CN^- detection in real water and food samples were verified. This work first investigated the quenching property of DNA-CuNPs and opened a new way to apply DNA-CuNPs in biosensor development.

3.2. Late-model biosensors

As most known, fluorescence emission of DNA-CuNPs is their outstanding properties, such as high red fluorescence and MegaStokes shifting, and most biosensors based on DNA-CuNPs are rooted in fluorescent assay. Undoubtedly, these have significantly facilitated the development of biosensors. However, there is also deficiency in DNA-CuNPs-based fluorescent biosensors, the focus barrier is from low photostability of DNA-CuNPs, thus it is difficult and challenging to conduct a long-time analysis with a label-free DNA-CuNPs fluorescent biosensor. Generally, cautious controls of experimental operations and conditions are required to achieve repeatable and stable performance. To compensate this limitation, efforts have been attempted to develop other biosensors based on exploiting late-model signal reading of DNA-CuNPs.

3.2.1. Electrochemical biosensors

By virtue of its advantages incuding high sensitivity, low cost and rapid response, the electrochemical technique has been widely used and intensely studied in construction of biosensors (Li et al., 2018b; Su et al., 2016). Various electrochemical biosensors based on DNA-CuNPs have been also developed for a series of targets including nucleic acids (Wang et al., 2015e, 2017b; Koo et al., 2017; Miao et al., 2018), proteins (Zhao et al., 2015a, 2015b, 2015c; Zhu et al., 2016), enzymes (Chen et al., 2018b; Hu et al., 2017), and small molecules (Sheng et al., 2017; Wang et al., 2017c). As the first example of electrochemical biosensors based on DNA-CuNPs, Dai group developed a microRNA sensor based on the electrocatalytic property of RNA/DNA heteroduplex-templated CuNPs (Wang et al., 2015e). They found that RNA/DNA heteroduplex could template the formation of CuNPs, which could electrocatalyze hydrogen peroxide (H_2O_2) reduction on an electrode surface, then the target miRNA could be detected by differential pulse voltammetry (DPV) electrochemical assay. Electrochemical biosensors based on DNA-CuNPs were also constructed for protein analysis. By using small molecule such as folate-linked DNA as probe, Zhao et al.

Table 5
Biosensors based on microenvironment modulation.

Target	Template type	Template length/bp	Read out	λ_{em}/nm (λ_{ex})/nm	Detection time/min	Detection limit	Linear range	Real sample	Ref
ATP	Poly T	18	Turn-on	630 (350)	15	10.29 nM	100 nM–100 μM	Cell extract	Zhou et al. (2016b)
Histone	dsDNA	20	Turn-on	580 (340)	20	8.3 nM	0.01–20 μM	–	Lian et al. (2017)
ALP	Poly T	30	Turn-on	650 (340)	90	3.5×10^{-2} U·L^{-1}	6×10^{-2}–6×10^{2} U·L^{-1}	Serum	Li et al. (2017)
ATP	dsDNA	18	Turn-off	596 (340)	20	28 nM	0.05–500 μM	Serum	Zhou et al. (2011)
SNPs	3WJ DNA	12	Turn-on (WT) Turn-off (MT)	594 (340)	–	–	–	Serum	Sun et al. (2017)
CEA	dsDNA	–	Turn-off	565 (340)	60	0.0065 ng mL^{-1}	0.01–2 ng mL^{-1}	Serum	Chen et al. (2018c)
ALP	dsDNA	–	Turn-on	565 (335)	60	0.1 nM	0.1–2.5 nM	Serum	Zhang et al. (2013b)
p53 DNA	dsDNA	24	Turn-on	471 (365)	180	52 pM	0.1–200 nM	Complex medium	Qiu et al. (2013)
L-histidine	dsDNA	22	Turn-off	580 (340)	–	5 μM	5–250 μM	Urine	Liu et al. (2013)
Biothiols	Poly T	25	Turn-on	615 (340)	120	12.5 nM (Cys) 15 nM (GSH) 20 nM (Hcy)	0–1000 nM	Serum	Zhang et al. (2015b)
L-histidine	dsDNA	25	Turn-off	565 (340)	5	20 nM	0.2–100 μM	Human urine	Wang et al. (2015d)
UDG	dsDNA	22	Turn-off	570 (340)	90	0.0005 U·mL^{-1}	0.001–0.1 U·mL^{-1}	Cell lysate	Cao et al. (2016)
Kojic acid	Poly T	30	Turn-off	615 (340)	10	30 nM	0.1–300 μM	Sauce and vinegar	Wang et al. (2016)
ALP	Poly T	30	Turn-on	625 (365)	0.5	5 mU·mL^{-1}	1–70 mU·mL^{-1}	–	Sun et al. (2016)
T4 PNKP	Poly T	30	Turn-off	520 (340)	15	0.25 U·mL^{-1}	0.25–25 U·mL^{-1}	Cell extract	Dong et al. (2016)
AChE	Poly T	40	Turn-off	600 (340)	35	0.05 mU·mL^{-1}	0.11–2.78 mU·mL^{-1}	Cell lysate	Ni et al. (2017)
IFN-γ	Poly T	22	Turn-off	615 (340)	10	1 pg mL^{-1}	10 pg mL^{-1}–4 ng mL^{-1}	Serum	Taghdisi et al. (2017)
HBV gene	Poly T	30	Turn-on	615 (340)	120	33.4 pM	0.1–80 nM	Serum	Xie et al. (2018)
Cys/His	Dumbbell DNA	40/30	Turn-off	630 (355)	30	98 pM (Cys) 1.6 nM (His)	0.01–10.0 μM (Cys) 0.05–40.0 μM (His)	Human urine	Gu and Cao (2018)

reported two electrochemical methods for highly sensitive and specific detection of protein based on target-dependent magnetic enrichment of DNA-CuNPs (Zhao et al., 2015a), or hybridization chain reaction(HCR)-assisted formation of copper nanoparticles (Fig. 8A) (Zhao et al., 2015b). Also, electrochemical aptasensors based on DNA-CuNPs were developed in the past years (Zhao et al., 2015c; Sheng et al., 2017), broadening the wide of analysis objects. In addition, endonuclease activity sensing was achieved by Chen et al. (2018b), a DNA duplex was designed and modified on a gold electrode, which could template the formation of CuNPs when in the absence of endonuclease, the formed CuNPs were dissolved by nitric acid and monitored by DPV measurements. As a function of introduction of endonuclease, the DNA duplex was recognized and digested, thus, CuNPs could not be templated and a declined DPV peak was observed to reflect the level of endonuclease activity. Furthermore, an electrochemical method for the detection of small biological molecule (e.g. glutathione, GSH) was developed by applying DNA-CuNPs as electrochemical reporters (Wang et al., 2017c).

3.2.2. SPR assay

Surface plasmon resonance (SPR) is one of the most important technique for the investigation of biomolecular recognitions, interactions and detections. Yuan et al. recently constructed a biosensor for DNA assay based on the *in situ* synthesis of CuNPs templated by poly-T sequences which were extended by terminal deoxynucleotidyl transferase, and synergistically with nano-effect deposition as the mass relay (Fig. 8B) (Yuan et al., 2017). When in the presence of the target DNA (tDNA), it hybridized with the capture probe, and then initiated the extension at the terminal of tDNA onto the surface of SPR chip, leading to generation of long poly T which can template the formation of CuNPs, finally the catechol violet (CV) was added for further signal amplification. This strategy displayed a good sensing performance with a low detection limit, and demonstrated a useful overlapping exploitation of DNA-CuNPs and molecular recognition for constructing unique SPR infrastructure.

3.2.3. ICPMS assay

Elemental mass spectrometric assay is an important sensing technique as a label-free manner, because it dose not depend on reporters' special properties such as colorimetric, fluorescent, electrochemical, and magnetic features. By virtue of its high spectral resolution, high sensitivity, wide linear range and low background interference, inductively coupled plasma mass spectrometry (ICPMS) has been a powerful technique for metal element analysis. Attractively, one metal nanoparticle contains a large number of metal atom, thus metal nanoparticles used as tags in ICPMS assay can improve the detection sensitivity. Recently, Lv group developed a label-free strategy for nucleic acid detection by directly measuring the intrinsic ^{63}Cu and ^{65}Cu stable isotopes inside dsDNA-CuNPs (Fig. 8C) (Liu et al., 2017), this strategy is sensitive in performance and simple in operation, opening up a new path to apply DNA-CuNPs as a new sensing reporter.

3.2.4. SERS assay

Surface-enhanced Raman scattering (SERS) as an analysis technique has been rapidly developed with the advancement of the theoretical understanding and experimental control of SERS. Metal nanomaterials such as gold and silver nanoparticles, are generally used to enhance the Raman scattering of signal units. We first investigated the SERS effect of DNA-CuNPs and its application in constructing biosensor (Fig. 8D) (Zhou et al., 2016a). As shown in Figure, a triple-helix molecular switch (THMS) was constructed as the probe and modified on the gold film (Zheng et al., 2011, 2012), an RNA site was embedded in the capture sequence while a poly T DNA was designed as a signal transduction section. When in the presence of the target circulating tumor DNA (ctDNA), and with the assistance of RNase HII, a lot of poly T sequences were released to template the formation of CuNPs. In addition, the released poly T could noncovalently absorb onto the surface of single-

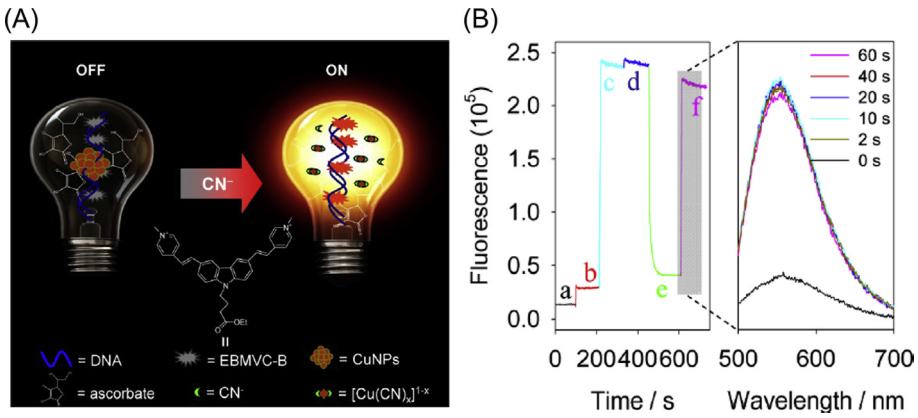

Fig. 7. Signaling based on quenching property of DNA-CuNPs. (A) Schematic Representation for Cyanide Monitoring based on the quenching effect of DNA-CuNPs on fluorophore EBMVC-B and an Elsner-Like Reaction between cyanide ion and CuNPs. (B) The left is the real-time monitoring of fluorescence with gradual addition of MOPS buffer (a), EBMVC-B (b), d(AT)20 (c), sodium ascorbate (d), Cu^{2+} (e) and CN^- (f); the right is the spectra change vs time after addition CN^- into the nanolamp system, which is corresponding to the gray process in the left. (Reproduced with permission from Ref. (Qing et al., 2016b). Copyright 2016, American Chemical Society).

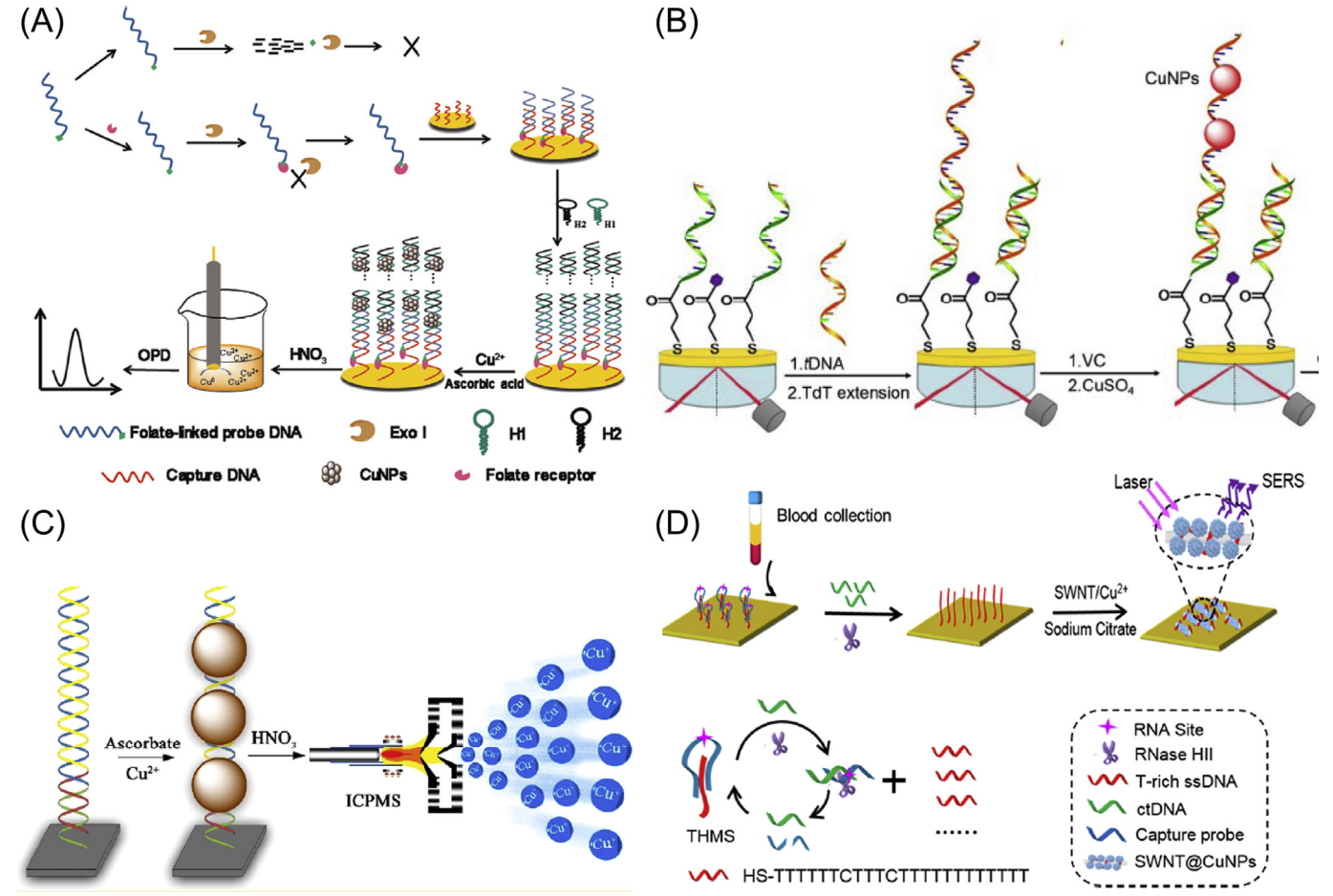

Fig. 8. Late-model biosensors based on DNA-CuNPs. (A) electrochemical detection of protein based on hybridization chain reaction-assisted formation of copper nanoparticles (Reproduced with permission from Ref. (Zhao et al., 2015b). Copyright 2015, Elsevier B.V.). (B) CuNPs templated by TdT-mediated DNA for SPR-DNA assay (Reproduced with permission from Ref. (Yuan et al., 2017). Copyright 2017, Elsevier B.V.). (C) ICPMS assay for target DNA based on hybridization chain reaction-assisted formation of copper nanoparticles (Reproduced with permission from Ref. (Liu et al., 2017). Copyright 2017, American Chemical Society). (D) SERS assay for highly sensitive detection of ctDNA in human blood based on RNase HII-assisted amplification and T-rich DNA-mediated growth of CuNPs to enhance the SERS signal of SWNTs. (Reproduced with permission from Ref. (Zhou et al., 2016a). Copyright 2016, American Chemical Society).

walled carbon nanotubes (SWNTs) through π-π stacking interactions (Yang et al., 2008; Zheng et al., 2015b). Significant SERS enhancement of SWNTs, including the radial breathing mode (RBM) and tangential mode (G-band), was found, this was due to the electromagnetic enhancement effect associated with the large local E field between CuNPs and SWNTs (Zhu et al., 2015b). As a result, this development provided an excellent strategy for highly sensitive biosensing such as target detection and clinical noninvasive liquid biopsy. DNA-CuNPs-based late-model biosensors are summarized in Table 6.

4. Summary and outlook

In this review, inspired by the development of DNA-CuNPs-based biosensors and their distinctive characteristics, we have summarized multiaspects of this field, from synthesis to application. DNA-templated copper nanoparticles exhibit obvious advantages in the development of biosensors: (1) Highly-efficient preparation, with simplicity in operation, rapidity in synthesis dynamics and low template concentration; (2) Good fluorescent properties, including red emission, large Stokes

Table 6
DNA-CuNPs-based late-model biosensors.

Type	Target	Template type	Read out	Detection time/min	Detection limit	Linear range	Real sample	Ref
Electrochemistry	MicroRNA 21	dsDNA	Turn-on	3	10 aM	10 pM–0.1 fM	Human blood	Wang et al. (2017b)
	MicroRNA	dsDNA	Turn-on	5	4.5×10^{-17} M	10^{-16}–10^{-13} M	Cell lysate	Miao et al. (2018)
	MicroRNA	Heteroduplex	Turn-on	5	8.2 fM	25–300 fM	Serum	Wang et al. (2015e)
	T1E4/miR-107/SChLAP1	Poly AT	Turn-on	0.5	100 fM (T1E4)	100 fM–100 pM (T1E4)	Urine	Koo et al. (2017)
					10 fM (miR-107)	10 fM–10 pM (miR-107)		
					100 fM (SChLAP1)	100 fM–100 pM (SChLAP1)		
	Folate receptor	dsDNA	Turn-on	20	7.8 pg mL^{-1}	0.01–100 ng mL^{-1}	Serum	Zhao et al. (2015a)
	Folate receptor	dsDNA	Turn-on	10	3 pg mL^{-1}	0.01–100 ng mL^{-1}	Serum	Zhao et al. (2015b)
	Thrombin	dsDNA	Turn-off	10	20.3 fM	100 fM–1 nM	Serum	Zhao et al. (2015c)
	PSA	Poly T	Turn-on	360	0.020 ± 0.001 fg mL^{-1}	0.05–500 fg mL^{-1}	Serum	Zhu et al. (2016)
	Endonuclease	dsDNA	Turn-off	5	10^{-3} U·mL^{-1}	10^{-3}–10 U·mL^{-1}	–	Chen et al. (2018b)
	TdT/*Bam*HI	Poly T	Turn-on	–	0.1 U·mL^{-1} (TdT)	0.5–160 U·mL^{-1} (TdT)	Serum and urine	Hu et al. (2017)
					0.004 U·mL^{-1} (*Bam*HI)	0.02–30 U·mL^{-1} (*Bam*HI)		
	Ractopamine	dsDNA	Turn-on	120	3×10^{-13} M	1×10^{-12}–3×10^{-7} M	Swine urine	Sheng et al. (2017)
	Glutathione	dsDNA	Turn-off	20	0.27 nM	1–1000 nM	–	Wang et al. (2017c)
SPR	DNA	Poly T	Turn-on	20	3.21 fM	10 fM–100 pM	–	Yuan et al. (2017)
ICPMS	DNA	dsDNA	Turn-on	60	4 pM	20–1000 pM	Serum	Liu et al. (2017)
SERS	ctDNA	Poly T	Turn-on	–	0.3 fM	10 fM–1.0 nM	Human blood	Zhou et al. (2016a)

shift, template length dependence and ion concentration dependence; (3) Environmental friendliness, copper is a an essential microelement for living organisms, it acts as an important cofactor of multiple functional proteins, thus CuNPs is more biosafer than other heavy metal-contained nanoparticles in application; (4) DNA-CuNPs is convenient to integrate with other functional units, such as aptamer-based recognition capability and enzyme-catalyzed signal amplification. Therefore, DNA-CuNPs-based biosensors have been intensely developed in the past years, and will be attractive in further.

Despite the remarkable progress of developing DNA-CuNPs-based biosensors, this research area is still in its early-stage, remaining great room for investigation and improvement. (1) On the fundamental facet, although there have been some studies on the relationship between the synthesis of DNA-CuNPs and the template DNA sequence, better understanding on the mechanism of sequence-dependent formation of DNA-CuNPs is also required, such as screening more DNA sequences that can template the formation of CuNPs and investigating more DNA configurations that can regulate optical properties of CuNPs. In addition, as demonstrated in previous reports, since the size and morphology is ununiform and variable, it is needed to theoretically control these physical geometry properties of DNA-CuNPs or develop strategies to improve the purity of this nanomaterials, which is importantly meaningful for developing more uniform and reliable biosensors. Thus, in a word, more systematically fundamental understanding on DNA-CuNPs is highly required and should be one of further research points in this field. (2) On the application facet, a relatively serious problem for CuNPs is its fragility in photostability, because of its tendency to undergo oxidation particularly at the small nanometer size geometry, which makes long-term detection difficult and challenging. It is essential to improve DNA-CuNPs' stability through various strategies including careful control of the experimental conditions, rational manipulation of microenvironment and physical package-based protection. Furthermore, signal transduction manner is too onefold, the signal generation of most DNA-CuNPs-based biosensors is from only CuNPs unit. There is a need to construct more abundant and higher efficient biosensors by integrating other functional units such as nanomaterials and molecular dyes. In addition, most developed DNA-CuNPs-based biosensors are fluorescent assays which are more susceptible to photostability than other analytical technologies, thus, it is a worthy way to develop more DNA-CuNPs-based biosensors via electrochemistry, ICPMS, SPR, and SERS, which may improve the reliable sensing and promote the practical applications.

Taken together, DNA-CuNPs as a useful tool for biochemical assay has opened a new path for constructing biosensors, we expect more effort will be made for this area and more developments will be brought.

Declaration of interest statement

None of the authors have any financial affiliations that may be perceived to have biased the presentation.

Acknowledgements

This work was supported in part by the financial support through the National Natural Science Foundation of China (21605008, 21575018, 21735001, 21705010), and the Natural Science Foundation of Hunan Province (2019JJ30025).

References

Becerril, H.A., Woolley, A.T., 2009. Chem. Soc. Rev. 38, 329–337.
Cai, Q., Ge, J., Xu, H., Zhang, L., Hu, Y., Huang, Z., Li, Z., 2017. Anal. Methods 9, 2710–2714.
Cao, M., Jin, Y., Li, B., 2016. Anal. Methods 8, 4319–4323.
Cao, Y., Wang, Z., Cao, J., Mao, X., Chen, G., Zhao, J., 2017a. Microchim. Acta 184, 3697–3704.

Cao, J., Wang, W., Bo, B., Mao, X., Wang, K., Zhu, X., 2017b. Biosens. Bioelectron. 90, 534–541.
Chen, J., Liu, J., Fang, Z., Zeng, L., 2012. Chem. Commun. 48, 1057–1059.
Chen, J., Ji, X., Tinnefeld, P., He, Z., 2016. ACS Appl. Mater. Interfaces 8, 1786–1794.
Chen, Z., Niu, Y., Cheng, G., Tong, L., Zhang, G., Cai, F., Chen, T., Liu, B., Tang, B., 2017. Analyst 142, 2781–2785.
Chen, Z., Liu, C., Cao, F., Ren, J., Qu, X., 2018a. Chem. Soc. Rev. 47, 4017–4072.
Chen, X., Yang, D., Tang, Y., Miao, P., 2018b. Analyst 143, 1685–1690.
Chen, M., Khusbu, F.Y., Ma, C., Wu, K., Zhao, H., Chen, H., Wang, K., 2018c. New J. Chem. 42, 13702–13707.
Chi, B.Z., Liang, R.P., Qiu, W.B., Yuan, Y.H., Qiu, J.D., 2017. Biosens. Bioelectron. 87, 216–221.
Dong, Z.Z., Zhang, L., Qiao, M., Ge, J., Liu, A.L., Li, Z.H., 2016. Talanta 146, 253–258.
Fang, X., Tan, W., 2009. Acc. Chem. Res. 43, 48–57.
Ge, J., Dong, Z., Zhang, L., Cai, Q., Bai, D., Li, Z., 2016a. RSC Adv. 6, 91077–91082.
Ge, J., Zhang, L., Dong, Z., Cai, Q., Li, Z., 2016b. Anal. Methods 8, 2831–2836.
Ge, J., Dong, Z.Z., Bai, D.M., Zhang, L., Hu, Y.L., Ji, D.Y., Li, Z.H., 2017. New J. Chem. 41, 9718–9723.
Goswami, N., Giri, A., Bootharaju, M.S., Xavier, P.L., Pradeep, T., Pal, S.K., 2011. Anal. Chem. 83, 9676–9680.
Gu, Z., Cao, Z., 2018. Anal. Bioanal. Chem. 410, 4991–4999.
Gwinn, E.G., O'Neill, P., Guerrero, A.J., Bouwmeester, D., Fygenson, D.K., 2008. Adv. Mater. 20, 279–283.
Han, B., Wang, E., 2012. Anal. Bioanal. Chem. 402, 129–138.
He, Y., Jiao, B., 2018. Sensor. Actuator. B Chem. 265, 387–393.
He, Z., Ye, T., Li, C., Su, C., Ji, X., Zheng, J., Tinnefeld, P., 2015. Chem. Commun. 51, 8644–8647.
Hu, Y., Wu, Y., Chen, T., Chu, X., Yu, R., 2013a. Anal. Methods 5, 3577–3581.
Hu, R., Liu, Y., Kong, R., Donovan, M.J., Zhang, X., Tan, W., Shen, G., Yu, R., 2013b. Biosens. Bioelectron. 42, 31–35.
Hu, W., Ning, Y., Kong, J., Zhang, X., 2015. Analyst 140, 5678–5684.
Hu, Y., Zhang, Q., Xu, L., Wang, J., Rao, J., Guo, Z., Wang, S., 2017. Anal. Bioanal. Chem. 409, 6677–6688.
Jia, X., Li, J., Han, L., Ren, J., Yang, X., Wang, E., 2012. ACS Nano 6, 3311–3317.
Jia, X., Li, J., Wang, E., 2013. Small 9, 3873–3879.
Jia, X., Yang, X., Li, J., Li, D., Wang, E., 2014. Chem. Commun. 50, 237–239.
Jiang, X., Du, B., Huang, Y., Zheng, J., 2018. Nano Today 21, 106–125.
Kennedy, T.A., MacLean, J.L., Liu, J., 2012. Chem. Commun. 48, 6845–6847.
Koo, K.M., Carrascosa, L.G., Trau, M., 2017. Nano Res 11, 940–952.
Koval, I.A., Gamez, P., Belle, C., Selmeczi, K., Reedijk, J., 2006. Chem. Soc. Rev. 35, 814–840.
Lai, Q., Liu, M., Gu, C., Nie, H., Xu, X., Li, Z., Yang, Z., Huang, S., 2016. Analyst 141, 1383–1389.
Li, J., Zhu, J., Xu, K., 2014. Trac. Trends Anal. Chem. 58, 90–98.
Li, H., Chang, J., Hou, T., Ge, L., Li, F., 2016. Talanta 160, 475–480.
Li, J., Si, L., Bao, J., Wang, Z., Dai, Z., 2017. Anal. Chem. 89, 3681–3686.
Li, J., Fu, W., Bao, J., Wang, Z., Dai, Z., 2018a. ACS Appl. Mater. Interfaces 10, 6965–6971.
Li, C., Hu, X., Lu, J., Mao, X., Xiang, Y., Shu, Y., Li, G., 2018b. Chem. Sci. 9, 979–984.
Li, X., Qing, Z., Li, Y., Zou, Z., Yang, S., Yang, R., 2019. ACS Omega 4, 793–800.
Lian, J., Liu, Q., Jin, Y., Li, B., 2017. Chem. Commun. 53, 12568–12571.
Lin, Z.Y., Wu, Y.T., Tseng, W.L., 2015. ACS Appl. Mater. Interfaces 7, 23708–23716.
Ling, Y., Li, J., Qu, F., Li, N., Luo, H., 2014. Microchim. Acta 181, 1069–1075.
Liu, J., 2014. Trac. Trends Anal. Chem. 58, 99–111.
Liu, J., Lu, Y., 2007. Angew. Chem. Int. Ed. 119, 7731–7734.
Liu, Y., Ai, K., Cheng, X., Huo, L., Lu, L., 2010. Adv. Funct. Mater. 20, 951–956.
Liu, G., Shao, Y., Ma, K., Cui, Q., Wu, Fei, Xu, S., 2012a. Gold Bull. 45, 69–74.
Liu, J., Chen, J., Fang, Z., Zeng, L., 2012b. Analyst 137, 5502–5505.
Liu, Y.R., Hu, R., Liu, T., Zhang, X.B., Tan, W., Shen, G.L., Yu, R.Q., 2013. Talanta 107, 402–407.
Liu, R., Wang, C., Xu, Y., Hu, J., Deng, D., Lv, Y., 2017. Anal. Chem. 89, 13269–13274.
Luo, L., Xu, F., Shi, H., He, X., Qing, T., Lei, Y., Tang, J., He, D., Wang, K., 2017. Talanta 169, 57–63.
Mao, Z., Qing, Z., Qing, T., Xu, F., Wen, L., He, X., He, D., Shi, H., Wang, K., 2015. Anal. Chem. 87, 7454–7460.
Miao, P., Zhang, T., Xu, J., Tang, Y., 2018. Anal. Chem. 90, 11154–11160.
Ng, E.W.M., Shima, D.T., Calias, P., Cunningham, E.T., Guyer, D.R., Adamis, A.P., 2006. Nat. Rev. Drug Discov. 5, 123–132.
Ni, P., Sun, Y., Jiang, S., Lu, W., Wang, Y., Li, Zhen, Li, Z., 2017. Sensor. Actuator. B Chem. 240, 651–656.
Ou, L., Li, X., Liu, H., Li, L., Chu, X., 2014. Anal. Sci. 30, 723–727.
Ou, L., Li, X., Li, L., Liu, H., Sun, A., Liu, K., 2015. Analyst 140, 1871–1875.
Park, K.W., Batule1, B.S., Kang, K.S., Park, K.S., Park, H.G., 2016. Nanotechnology 27, 425502.
Park, K.W., Lee, C.Y., Batule, B.S., Park, K.S., Park, H.G., 2018. RSC Adv. 8, 1958–1962.
Peng, F., Liu, Z., Li, W., Huang, Y., Nie, Z., Yao, S., 2015. Anal. Methods 7, 4355–4361.
Peng, J., Ling, J., Tan, Y.Y., Jing, C.J., Li, X.J., Chen, L.Q., Cao, Q.E., 2017. Spectrosc. Lett. 50, 137–142.
Petty, J.T., Zheng, J., Hud, N.V., Dickson, R.M., 2004. J. Am. Chem. Soc. 126, 5207–5212.
Plastino, J., Green, E.L., Sanders-Loehr, J., Klinman, J.P., 1999. Biochemistry 38, 8204–8216.
Qing, Z., He, X., He, D., Wang, K., Xu, F., Qing, T., Yang, X., 2013a. Angew. Chem. Int. Ed. 52, 9719–9722.
Qing, Z., He, X., Qing, T., Wang, K., Shi, H., He, D., Zou, Z., Yan, L., Xu, F., Ye, X., Mao, Z., 2013b. Anal. Chem. 85, 12138–12143.
Qing, T., Qing, Z., Mao, Z., He, X., Xu, F., Wen, L., He, D., Shi, H., Wang, K., 2014a. RSC Adv. 4, 61092–61095.
Qing, Z., Mao, Z., Qing, T., He, X., Zou, Z., He, D., Shi, H., Huang, J., Liu, J., Wang, K., 2014b. Anal. Chem. 86, 11263–11268.
Qing, Z., Qing, T., Mao, Z., He, X., Wang, K., Zou, Z., Shi, H., He, D., 2014c. Chem. Commun. 50, 12746–12748.
Qing, Z., Zhu, L., Yang, S., Cao, Z., He, X., Wang, K., Yang, R., 2016a. Biosens. Bioelectron. 78, 471–476.
Qing, Z., Hou, L., Yang, L., Zhu, L., Yang, S., Zheng, J., Yang, R., 2016b. Anal. Chem. 88, 9759–9765.
Qing, Z., Zhu, L., Li, X., Yang, S., Zou, Z., Guo, J., Cao, Z., Yang, R., 2017a. Environ. Sci. Technol. 51, 11884–11890.
Qing, T., He, X., He, D., Ye, X., Shangguan, J., Liu, J., Yuan, B., Wang, K., 2017b. Biosens. Bioelectron. 94, 456–463.
Qing, Z., Zhu, L., Hou, L., Zou, Z., Yang, S., Yang, R., 2018. Sci. China Chem. 61, 1630–1636.
Qiu, S., Li, X., Xiong, W., Xie, L., Guo, L., Lin, Z., Qiu, Bin, Chen, G., 2013. Biosens. Bioelectron. 41, 403–408.
Retnakumari, A., Setua, S., Menon, D., Ravindran, P., Muhammed, H., Pradeep, T., Nair, S., Koyakutty, M., 2010. Nanotechnology 21, 055103.
Rotaru, A., Dutta, S., Jentzsch, E., Gothelf, E., Mokhir, A., 2010. Angew. Chem. Int. Ed. 49, 5665–5667.
Schultz, D., Gardner, K., Oemrawsingh, S.S., Markešević, N., Olsson, K., Debord, M., Bouwmeester, D., Gwinn, E., 2013. Adv. Mater. 25, 2797–2803.
Shang, L., Dong, S., Nienhaus, G.U., 2011. Nano Today 6, 401–418.
Sheng, F., Zhang, X., Wang, G., 2017. J. Mater. Chem. B. 5, 53–61.
Song, Q., Shi, Y., He, D., Xu, S., Ouyang, J., 2015. Chem. Eur J. 21, 2417–2422.
Song, Q., Wang, R., Sun, F., Chen, H., Wang, Z., Na, N., Ouyang, J., 2017a. Biosens. Bioelectron. 87, 760–763.
Song, Q., Yang, L., Chen, H., Zhang, R., Na, N., Ouyang, J., 2017b. Talanta 174, 444–447.
Song, C., Hong, W., Zhang, X., Lu, Y., 2018a. Analyst 143, 1829–1834.
Song, W., Zhang, N., Luan, Z., Zhang, X., He, P., 2018b. RSC Adv. 8, 15248–15252.
Su, J., Gao, F., 2013. Mater. Lett. 108, 58–61.
Su, J., Gao, F., Hou, L., 2013. Mater. Lett. 92, 206–209.
Su, S., Wu, Y., Zhu, D., Chao, J., Liu, X., Wan, Y., Su, Y., Zuo, X., Fan, C., Wang, L., 2016. Small 12, 3794–3801.
Sun, J., Hu, T., Xu, X., Wang, L., Yang, X., 2016. Nanoscale 8, 16846–16850.
Sun, F., You, Y., Liu, J., Song, Q., Shen, X., Na, N., Ouyang, J., 2017. Chem. Eur J. 23, 6979–6982.
Taghdisi, S.M., Danesh, N.M., Ramezani, M., Yazdian-Robati, R., Abnous, K., 2017. Anal. Chim. Acta 984, 162–167.
Tanaka, S., Miyazaki, J., Tiwari, D.K., Jin, T., Inouye, Y., 2011. Angew. Chem. Int. Ed. 50, 431–435.
Tao, Y., Li, M., Ren, J., Qu, X., 2015. Chem. Soc. Rev. 44, 8636–8663.
Vosch, T., Antoku, Y., Hsiang, J.C., Richards, C.I., Gonzalez, J.I., Dickson, R.M., 2007. Proc. Natl. Acad. Sci. U.S.A. 104, 12616–12621.
Wang, K., Tang, Z., Yang, C., Kim, Y., Fang, X., Li, W., Wu, Y., Medley, C.D., Cao, Z., Li, J., Colon, P., Lin, H., Tan, W., 2009. Angew. Chem. Int. Ed. 48, 856–870.
Wang, Y., Cui, Y., Liu, R., Wei, Y., Jiang, X., Zhu, H., Gao, L., Zhao, Y., Chai, Z., Gao, X., 2013a. Chem. Commun. 49, 10724–10726.
Wang, X., Yin, B., Ye, B., 2013b. RSC Adv. 3, 8633–8636.
Wang, H., Zhang, H., Chen, Y., Huang, K., Liu, Y., 2015a. Sensor. Actuator. B Chem. 220, 146–153.
Wang, H., Zhang, H., Chen, Y., Li, Y., Gan, T., 2015b. RSC Adv. 5, 77906–77912.
Wang, H., Zhang, H., Chen, Y., Liu, Y., 2015c. Biosens. Bioelectron. 74, 581–586.
Wang, H.B., Zhang, H.D., Chen, Y., Liu, Y.M., 2015d. New J. Chem. 39, 8896–8900.
Wang, Z., Si, L., Bao, J., Dai, Z., 2015e. Chem. Commun. 51, 6305–6307.
Wang, H., Chen, Y., Li, Y., Liu, Y., 2016. Anal. Methods 8, 8322–8328.
Wang, Y., Liu, J., Duan, L., Liu, S., Jiang, J., 2017a. Microchim. Acta 184, 4183–4188.
Wang, Y., Zhang, X., Zhao, L., Bao, T., Wen, W., Zhang, X., Wang, S., 2017b. Biosens. Bioelectron. 98, 386–391.
Wang, Z., Han, P., Mao, X., Yin, Y., Cao, Y., 2017c. Sensor. Actuator. B Chem. 238, 325–330.
Wing, R., Drew, H., Takano, T., Broka, C., Tanaka, S., Itakura, K., Dickerson, R.E., 1980. Nature 287, 755–758.
Wu, X., He, X., Wang, K., Xie, C., Zhou, B., Qing, Z., 2010. Nanoscale 2, 2244–2249.
Xie, J., Zheng, Y., Ying, J., 2009. J. Am. Chem. Soc. 131, 888–889.
Xie, Q., Shi, D., Wan, J., Zhang, X., Wang, G., 2018. Anal. Methods 10, 2614–2622.
Xiong, Y., Gao, B., Wu, K., Wu, Y., Chai, Y., Huang, X., Xiong, Y., 2018. Nanoscale 10, 19890–19897.
Xu, F., Shi, H., He, X., Wang, K., He, D., Guo, Q., Qing, Z., Yan, L., Ye, X., Li, D., Tang, J., 2014. Anal. Chem. 86, 6976–6982.
Xu, F., Luo, L., Shi, H., He, X., Lei, Y., Tang, J., He, D., Qiao, Z., Wang, K., 2018. Anal. Chim. Acta 1010, 54–61.
Yang, R., Jin, J., Chen, Y., Shao, N., Kang, K., Xiao, Z., Tang, Z., Wu, Y., Zhu, Z., Tan, W., 2008. J. Am. Chem. Soc. 130, 8351–8358.
Yang, X.H., Sun, S., Liu, P., Wang, K.M., Wang, Q., Liu, J.B., Huang, J., He, L.L., 2014. Chin. Chem. Lett. 25, 9–14.
Yang, L., Qing, Z., Liu, C., Tang, Q., Li, J., Yang, S., Zheng, J., Yang, R., Tan, W., 2016. Anal. Chem. 88, 9285–9292.
Yin, J., Liu, F., Fan, T., Ren, Y., Jiang, Y., 2018. Sensor. Actuator. B Chem. 276, 499–506.
Yuan, P., Deng, S., Zheng, C., Cosnier, S., Shan, D., 2017. Biosens. Bioelectron. 97, 1–7.
Zhang, L., Wang, E., 2014. Nano Today 9, 132–157.
Zhang, L., Zhao, J., Zhang, H., Jiang, J., Yu, R., 2013a. Biosens. Bioelectron. 44, 6–9.
Zhang, L., Zhao, J., Duan, M., Zhang, H., Jiang, J., Yu, R., 2013b. Anal. Chem. 85, 3797–3801.
Zhang, Y., Zhu, C., Zhang, L., Tan, C., Yang, J., Chen, B., Wang, L., Zhang, H., 2014. Small

11, 1385–1389.
Zhang, H., Lin, Z., Su, X., 2015a. Talanta 131, 59–63.
Zhang, L., Cai, Q.Y., Li, J., Ge, J., Wang, J.Y., Dong, Z.Z., Li, Z.H., 2015b. Biosens. Bioelectron. 69, 77–82.
Zhao, J., Lv, Y., Kang, M., Wang, K., Xiang, Y., 2015a. Analyst 140, 7818–7822.
Zhao, J., Hu, S., Cao, Y., Zhang, B., Li, G., 2015b. Biosens. Bioelectron. 66, 327–331.
Zhao, J., Xin, M., Cao, Y., Yin, Y., Shu, Y., Ma, W., 2015c. Anal. Chim. Acta 860, 23–28.
Zhao, H., Dong, J., Zhou, F., Li, B., 2017. Sensor. Actuator. B Chem. 238, 828–833.
Zheng, J., Li, J., Jiang, Y., Jin, J., Wang, K., Yang, R., Tan, W., 2011. Anal. Chem. 83, 6586–6592.
Zheng, J., Jiao, A., Yang, R., Li, H., Li, J., Shi, M., Ma, C., Jiang, Y., Deng, L., Tan, W., 2012. J. Am. Chem. Soc. 134, 19957–19960.
Zheng, J., Yang, R., Shi, M., Wu, C., Fang, X., Li, Y., Li, J., Tan, W., 2015a. Chem. Soc. Rev. 44, 3036–3055.
Zheng, J., Bai, J., Zhou, Q., Li, J., Li, Y., Yang, J., Yang, R., 2015b. Chem. Commun. 51, 6552–6555.
Zhou, Z., Du, Y., Dong, S., 2011. Anal. Chem. 83, 5122–5127.
Zhou, Q., Zheng, J., Qing, Z., Zheng, M., Yang, J., Yang, S., Ying, L., Yang, R., 2016a. Anal. Chem. 88, 4759–4765.
Zhou, S., Zhang, L., Cai, Q., Dong, Z., Geng, X., Ge, J., Li, Z., 2016b. Anal. Bioanal. Chem. 408, 6711–6717.
Zhou, F., Cui, X., Shang, A., Lian, J., Yang, L., Jin, Y., Li, B., 2017. Microchim. Acta 184, 773–779.
Zhu, G., Zheng, J., Song, E., Donovana, M., Zhang, K., Liu, C., Tan, W., 2013. Proc. Natl. Acad. Sci. U.S.A. 110, 7998–8003.
Zhu, X., Shi, H., Shen, Y., Zhang, B., Zhao, J., Li, G., 2015a. Nano Res 8, 2714–2720.
Zhu, Y., Jiang, X., Wang, H., Wang, S., Wang, H., Sun, B., Su, Y., He, Y., 2015b. Anal. Chem. 87, 6631–6638.
Zhu, Y., Wang, H., Wang, L., Zhu, J., Jiang, W., 2016. ACS Appl. Mater. Interfaces 8, 2573–2581.
Zhu, L., Qing, Z., Hou, L., Yang, S., Zou, Z., Cao, Z., Yang, R., 2017. ACS Sens. 2, 1198–1204.